# The cardiac muscle cell

**Nicholas J. Severs**

**Summary**

**The cardiac myocyte is the most physically energetic cell in the body, contracting constantly, without tiring, 3 billion times or more in an average human lifespan. By coordinating its beating activity with that of its 3 billion neighbours in the main pump of the human heart, over 7,000 litres of blood are pumped per day, without conscious effort, along 100,000 miles of blood vessels. A detailed picture of the membrane organisation of the cardiac muscle cell underpins our understanding of how the electrical impulse, generated within the heart, stimulates coordinated contraction of the cardiac chambers. This article highlights, with the aid of modern cellular imaging methods, key components of the membrane machinery responsible for coupling electrical excitation and contraction in the cardiomyocyte, focusing on plasma membrane/sarcoplasmic reticulum and plasma membrane/plasma membrane junctions.** ***BioEssays*** **22:188–199, 2000.** 

## Introduction: "Thought is impossible without an image." (Aristotle, 325 BC)

My first glimpse of cell structure on the fluorescent screen of an electron microscope during an undergraduate practical in the early 1970s sparked an abiding interest, which despite the range of cell biological, molecular, biochemical, and physiological approaches later integrated into my research, has never dimmed. Mechanistic data are, of course, essential, but to me, being able to see the structural organisation of the cell at first hand was, and still is, a key step in making sense of functional concepts—getting to grips with how cells really work. Even to those whose acquaintanceship with cell structure is limited to standard text-book electron micrographs, my favourite cell, the cardiac myocyte, provides a strikingly clear example—a cell so crammed full of striated myofibrils and mitochondria that its supreme specialisation for energy-dependent contraction is grasped at a glance (Fig. 1A). Persuasive as such traditional thin-section electron-microscopic images may seem, however, they in fact give us only part of the picture. What they fail to bring to the fore is the presiding role of the myocyte's membranes in orchestrating its contraction/relaxation cycle.

National Heart and Lung Institute, Imperial College of Science, Technology and Medicine, Royal Brompton Hospital, Sydney Street, London SW3 6NP, England. E-mail: n.severs@ic.ac.uk
Funding agencies: Wellcome Trust, British Heart Foundation.

Contraction of the cardiac chambers is brought about by the orderly spread of action potentials throughout the heart. Each wave of electrical excitation spreads rapidly along the plasma membranes of adjoining cardiac muscle cells, triggering release of calcium from an intracellular membrane-bound compartment, the sarcoplasmic reticulum, which in turn stimulates contraction of the myofibrils. Integration of the electrical and mechanical properties of each and every myocyte within the heart is achieved by specialised portions of the plasma membrane that link neighbouring cells, the intercalated disks. With the aid of state-of-the-art cellular imaging techniques, we now have unprecedented opportunities to appreciate how the exquisitely specialised membrane microanatomy of the cardiomyoyte co-ordinates these processes.

## Membranes at centre stage

For many years, ultrastructural studies on membranes relied on the two-dimensional images provided by thin sections of plastic-embedded samples like that shown in Figure 1A. Alternatively, fragments of membranes, entirely removed from their normal cellular context, were examined by negative staining. A major breakthrough came in the mid-1960s with an entirely different approach to imaging membranes, the technique of freeze-fracture electron microscopy (for review see Ref. 1). Through a chance meeting with Stanley Bullivant in London in 1973, I started playing with this technique, then in its heyday, using simple, homemade equipment. At that time, membranes were the focus of great excitement in cell biology; the fluid mosaic model of membrane structure, which we now take for granted, had only recently been proposed, and the key questions of the day centred on the role of membranes in regulating cell activities. As one contemporary textbook put it: "Suddenly it is all membranes. Activities, speculations and enthusiasms that were devoted to informational macromolecules in the decade between 1955-1965 have now swung towards problems of biologic membranes".[2] How the pendulum has since swung back!

Freeze-fracture revolutionized the study of cell structure by giving us spectacular *en face* views of membranes, disclosing details of their architecture at macromolecular resolution. A new three-dimensional perspective of cellular organisation was opened—one in which membranes, viewed in their natural setting *in situ* in the cell and tissue, sprang into pre-eminence (Fig. 1B). Whereas standard thin-section electron microscopy emphasised features such as the "unit membrane" structure common to all membranes, freeze-fracture revealed a wealth of structural diversity between

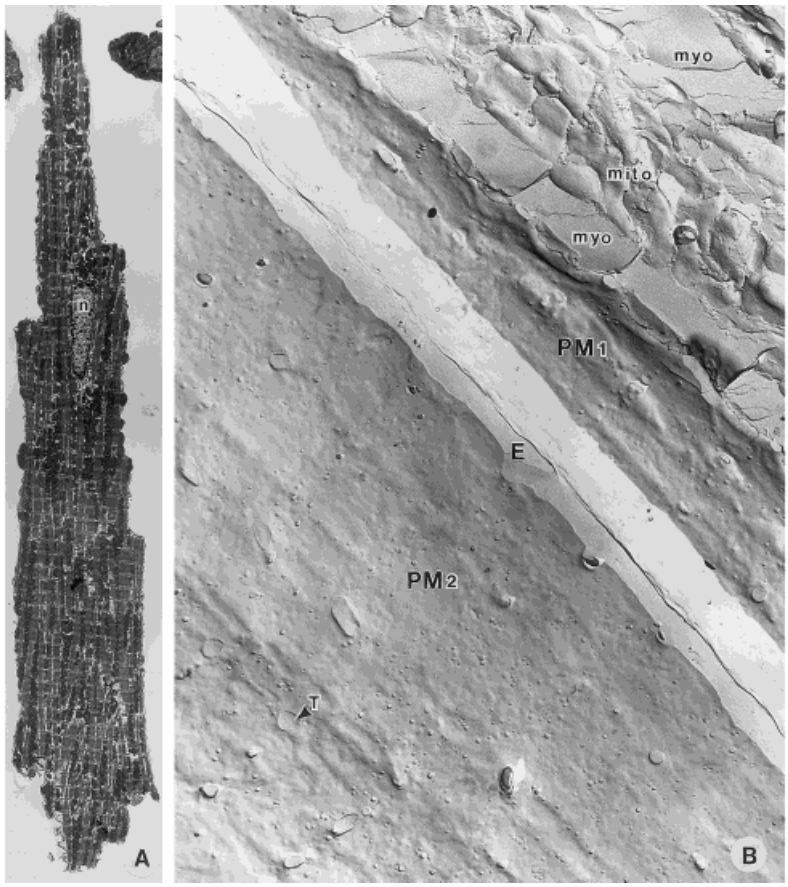


**Figure 1.** Electron-microscopic views of cardiac muscle.

**(A)** Thin-section electron micrograph of a single ventricular cardiomyocyte. The cell is packed full of striated myofibrils (the contractile apparatus) with rows of interposed mitochondria. n, nucleus. × 1,500.

**(B)** Freeze-fracture electron micrograph of cardiac muscle, showing portions of two adjacent cardiomyocytes. From the top right, the fracture plane has crossed through the tip of one cell, revealing a row of mitochondria (mito) predominantly fractured along their membranes, with spaces occupied by myofibrils (myo) on either side. The fracture has then entered the plasma membrane at the lower side of the cell (PM1), splitting it to give an *en face* view, before crossing a thin layer of extracellular matrix (E), and entering the plasma membrane of a second cell at the lower left of the picture (PM2). Here, the fracture has scooped out the entire cell, leaving the outermost half-membrane leaflet of the plasma membrane for viewing *en face*. T, transverse tubule opening. For a higher magnification view of plasma membrane structure, see Figure 3. × 11,000. Reduced to 60% for publication.

and within membranes. The technique works because fracturing a biological sample at low temperature frequently results in membranes being split along a plane in their hydrophobic core; structural detail of the resultant topography is revealed by casting a very fine platinum-carbon replica which is viewed (without the sample) in the transmission electron microscope. Apart from disclosing proteins penetrating the hydrophobic core of the membrane, the ability to visualise surface structure, to examine how specific channels and receptors are organised, and to capture transient, dynamic membrane-mediated events as they happen, ensured that the host of low temperature and replication techniques that grew alongside and from freeze-fracture were to have a wide-ranging and enduring impact in membrane biology.[1]

## Combining images of membranes with maps of their composition

It was in this setting, then, that I entered the membrane field, initially working on the nuclear envelope and then in the late 1970s on membranes of the mammalian urinary bladder with Marian Hicks at the Middlesex Hospital Medical School. There I met Trevor Powell, who at that time had just started isolating whole intact cardiac muscle cells for electrophysiological studies. Though my initial look at these cells was not especially enlightening, my interest in the myocyte intensified when, in 1979, seeking a more secure base from which to operate, I joined the Cardiothoracic Institute (now National Heart and Lung Institute, Imperial College School of Medicine). The two decades that have since elapsed have witnessed a revolution in cellular imaging techniques, now making it possible to pinpoint, at high resolution, the precise positions and spatial organisation of proteins of known identity, and to build this information into the overall structural template established by traditional techniques. Among key developments were the introduction of immunogold labelling—the use of minute (nm-sized) colloidal gold particles as electron-dense, easy-to-see markers, in conjunction with antibodies, for high resolution localization of specific proteins—and low denaturation techniques for electron-microscopical processing, which combine acceptable ultrastructural preservation with epitope retention (and hence the ability of antibody probes to detect their in-

tended targets).[3,4] Physical fixation by rapid freezing as an alternative to the standard epitope-destroying chemical fixatives, and other low temperature techniques, found wide application in a range of procedures (e.g., cryosectioning, freeze-substitution, and low temperature embedding in hydrophillic resins), which permitted examination of immunogold labelled thin sections. But from the point of view of membranes, the full potential of immunogold labelling only became realised with the invention of effective methods in freeze-fracture cytochemistry, pioneered through the 1980s by Pedro Pinto da Silva, culminating in the ability to piece together at high resolution the patchwork of compositional domains that determine membrane function[5,6] (for reviews see refs. 5 and 6). Interest in the microstructural basis of cell function across a broad front has, at the same time, been reinforced by the need to ascribe functions to the ever increasing number of newly identified gene products. And with the ever-wider accessibility of off-the-shelf and custom-designed antibodies, the means now exist to localize virtually any protein of interest at will. Add to this the renaissance of light microscopy in the form of confocal laser scanning microscopy,[7] with its capabilities for localization, three-dimensional reconstruction, real time imaging, and much more besides, we are now better placed than ever to unify understanding of cellular organisation from the level of the tissue, through that of the cell, organelle, and membrane system, down to the details of the membrane mosaics that drive individual cellular functions.

## Micromorphological sketch of the cardiac muscle cell and its plasma membrane structure

To see how these developments have influenced our understanding of the functional morphology of the myocyte's membranes, let us begin with an overview of the cell's structure. As Figure 1A illustrates, the typical contractile ("working") myocyte of the ventricles is an elongated cell, typically 100 to 150 μm in length and 20 to 35 μm in width. The contractile myofilaments (actin, myosin, and associated proteins) are packed together to form the familiar striated myofibrils that fill most of the cell. As individual myofibrils vary in length, myocytes have a variable branching morphology, best appreciated from three-dimensional confocal reconstructions (Fig. 2A). The myofibrils are held in position by scaffold-like webs of desmin filaments, rather like pistons in a woven cylinder. One anchorage site for the desmin is provided by costameres, transversely oriented rib-like plasma membrane plaques, enriched in vinculin, which circumscribe the lateral surface of the myocyte (Fig. 2B). Apart from maintaining the spatial organisation of the contractile apparatus, the costameres mechanically couple the cells laterally to the extracellular matrix. Linking to the costameres, closely applied to the entire cytoplasmic aspect of the lateral plasma membrane, is the membrane skeleton, formed from networks of peripheral membrane proteins such as spectrin and dystrophin[8] (Fig. 2C). The membrane skeleton strengthens the plasma membrane against the rigours of contraction and further contributes to lateral force transmission. The costameres, membrane skeleton, and cytoskeleton are linked to constituents of the extracellular matrix by sets of integral membrane proteins, notably integrins and components of the dystrophin-glycoprotein complex[9] (Fig. 2C).

Adjacent to the costameres and the Z bands of the superficial myofibrils, long finger-like extensions of the plasma membrane, the transverse tubules, penetrate deeply into the cell, stabilised by a coat of vinculin and dystrophin continuous with that at the surface (Fig. 2B and C). Planar freeze-fracture views reveal expanses of the plasma membrane punctuated with regular arrays of transverse tubule openings (Fig. 3A). Scattered over the intervening membrane areas are caveolae, small cholesterol-enriched membrane invaginations in which signal-transducing and water channel proteins are concentrated.[10,11] At higher magnification, the freeze-fractured plasma membrane is seen to be studded with abundant, scattered intramembrane particles, 3 to 10 nm in diameter (Fig. 3B); these particles represent the complement of specific channels, ion exchangers, carriers, receptors, and other integral proteins that endow the plasma membrane of the cardiomyocyte with its unique electrical, transport, and signal detection/transduction properties. Identification of these proteins, and analysis of their spatial organisation, is now readily achievable by freeze-fracture cytochemistry (Fig. 3C and D). For example, the technique of fracture-label combined with double immunogold marking demonstrates, at the plasma membrane interface, a direct molecular interaction between the carboxyl-terminal domains of dystrophin (a peripheral membrane protein of the membrane skeleton) and β-dystroglycan (an integral membrane protein which in turn binds to laminin via α-dystroglycan on the extracellular side of the membrane)[9] (Fig. 3C).

## Sarcoplasmic reticulum and its coupling to the plasma membrane

Within the cell, each myofibril is surrounded by a network of interconnecting membranous tubules, the sarcoplasmic reticulum (SR) (Fig. 4A). At multiple sites within this network, the membranes broaden out to form flattened sacs, the junctional SR cisternae, which press tightly against the peripheral plasma membrane and transverse tubules (Figs. 4B & 4C). Upon depolarisation, influx of calcium through L-type calcium channels in the plasma membrane triggers the opening of calcium release channels in the junctional SR membrane, resulting in the major release of calcium into the cytoplasm that triggers myofibril contraction (*calcium-induced calcium release*). Following contraction, a $Ca^{2+}$ ATPase enzyme in the network of non-junctional SR surrounding the myofibrils, visualised by freeze-fracture in Figure 4A, rapidly pumps the calcium back into the SR lumen, causing the myofibrils to relax. The freeze-fracture cytochemical technique, label-fracture, demonstrates that

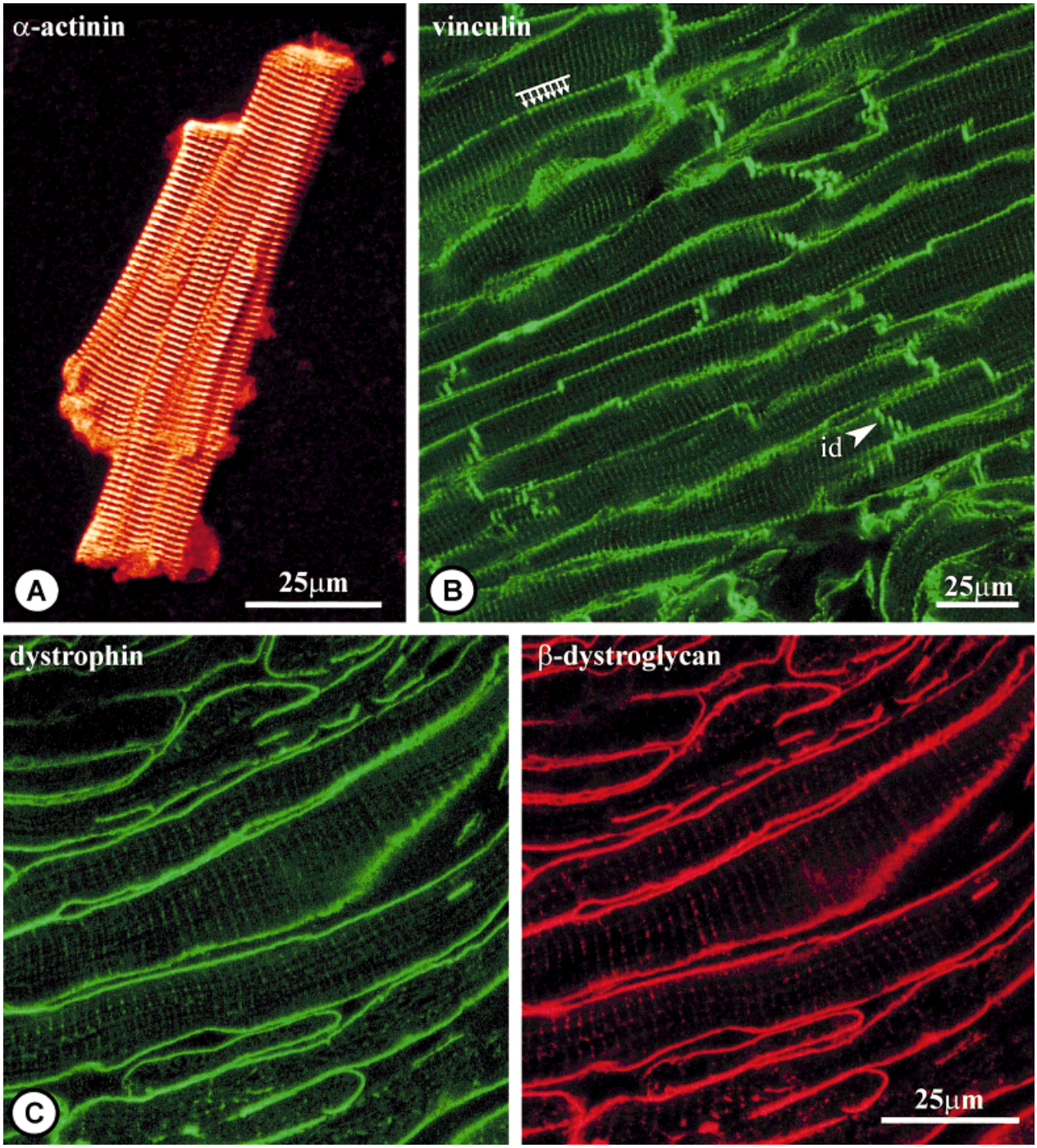


**Figure 2.** Confocal microscopy of cardiac muscle.

**(A)** Single ventricular myocyte viewed by confocal microscopy. Image prepared by combining a stack of serial optical sections through the cell. Myofibrils (seen as striations) visualised by immunostaining with an antibody against α-actinin (a component of the myofibril Z-bands).

**(B)** Distribution of vinculin in a section of cardiac muscle revealed by immunofluorescence labelling. The image shows numerous cells like that in panel (A), joined together at intercalated disks (id). Vinculin is seen as a series of bright dots along the lateral surfaces of the plasma membrane (series of small arrows), marking the sites of costameres. Vinculin extends from the surface plasma membrane along the transverse tubule membranes penetrating into the cell (seen as striations) and is also abundant in the transverse segments of the disk, where the myofibrils join the plasma membrane via fasciae adherentes junctions.

**(C)** Immunoconfocal localization of dystrophin (a peripheral membrane protein) and β-dystroglycan (an integral membrane protein) by double labelling. Both these proteins show a continuous distribution at the lateral plasma membrane in the rodent myocardium viewed here, and form part of the structure of the transverse tubules penetrating into the cell. Unlike vinculin, dystrophin, and β-dystroglycan are not present at the intercalated disks. (Micrographs by Shirley Stevenson and Stephen Rothery).

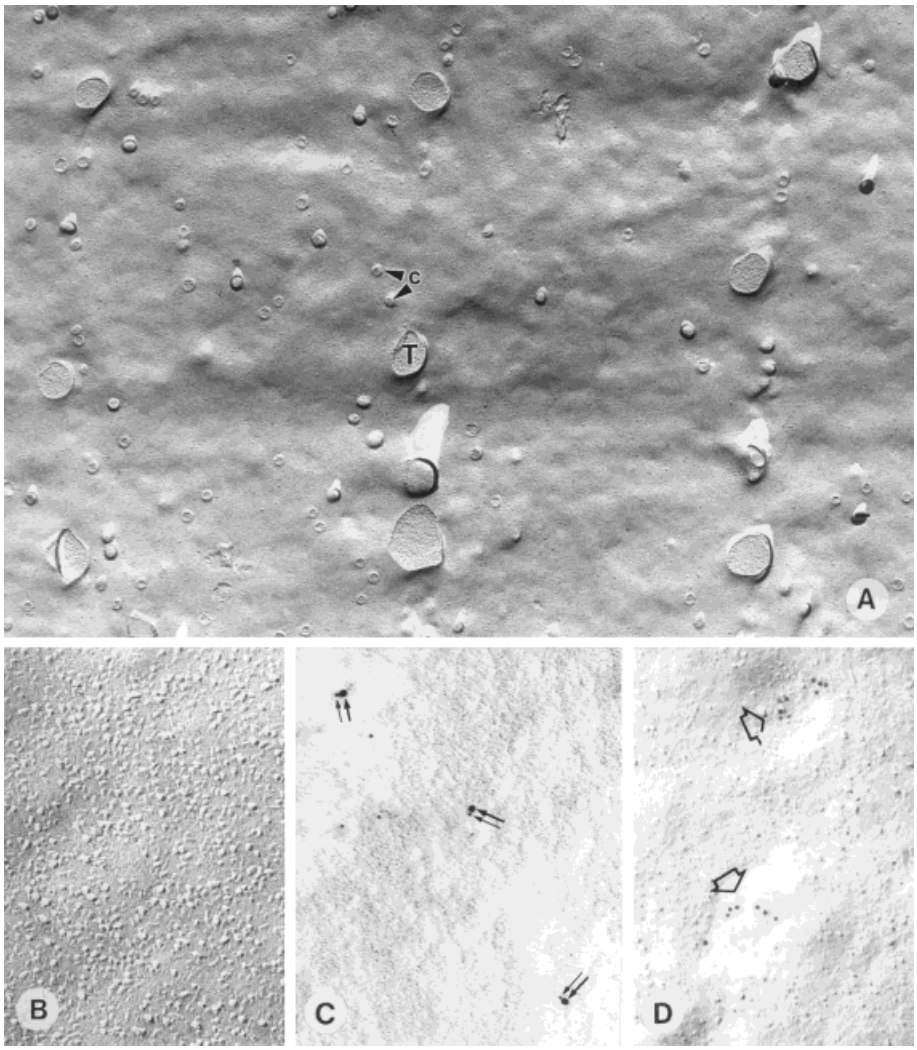


**Figure 3.** Freeze-fracture images of plasma membrane structure and composition.

**(A)** Planar freeze-fracture view of the plasma membrane, showing regular arrays of transverse tubule openings (T), and smaller vesicular structures, the caveolae (c). To understand this image, imagine yourself inside the cell looking towards its plasma membrane surface, but with the cell itself and the innermost half-membrane leaflet of the plasma membrane fractured away. All that remains is the outermost half-membrane leaflet, with the extracellular space beneath. At the site of the transverse tubule openings, the plasma membrane curves upwards; before freeze-fracture, these were finger-like extensions of the plasma membrane projecting upwards, towards you, at right angles to the plane of the page. Regular arrays of transverse tubule openings like those shown are confined to limited areas of the surface. × 29,000. Reduced to 70% for publication.

**(B)** High magnification freeze-fracture views disclose a heterogeneous collection of particles (3-10 nm in diameter), which represent the integral proteins of the membrane. × 140,000. Reduced to 70% for publication.

**(C)** Direct molecular interaction between the carboxyl-terminal domains of dystrophin and β-dystroglycan is demonstrated by the freeze-fracture cytochemical technique, fracture-label (pairs of arrows: large gold markers, β-dystroglycan; small gold, dystrophin). (Micrograph by Shirley Stevenson). × 130,000. Reduced to 70% for publication.

**(D)** L-type calcium channels are shown by the freeze-fracture cytochemical technique, label-fracture, to be aggregated in the plasma membrane (arrows); mathematical analysis confirms true clustering.[12,13] (From guinea-pig ventricular myocyte; micrograph by Yoshiko Takagishi). × 80,000. Reduced to 70% for publication.

L-type calcium channels are organised in discrete clusters in the plasma membrane (Fig. 3D), and labelling of ultrathin cryosections cut across the cell shows these clusters to face underlying junctional SR cisternae.[12,13] Such a close spatial apposition of L-type calcium channels (in both the peripheral plasma membrane and transverse tubules) to calcium re-

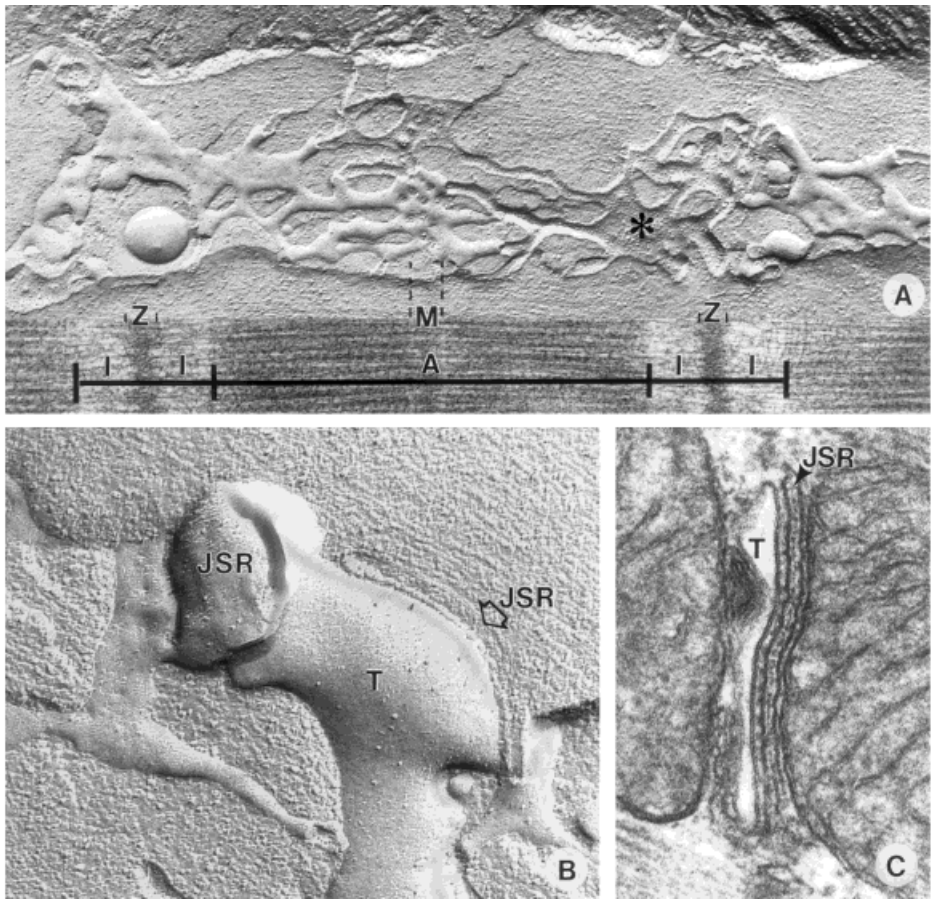


**Figure 4.** Sarcoplasmic reticulum and its relationships with transverse tubules.

**(A)** Freeze-fracture view of the sarcoplasmic reticulum (SR) network that surrounds each myofibril (the thin-section image below shows alignment of the SR with respect to the sarcomere bands). Structurally distinct regions of the sarcoplasmic reticulum are apparent in this example; a cisternal element with "pores" in the centre of the sarcomere (in line with the M band) joins to longitudinal tubules with relatively few interconnections extending on either side over the A-band region, with more elaborate interconnections at the I and Z-band level. The numerous particles visible on the protoplasmic fracture face of the SR membrane (*) represent the $Ca^{2+}$ATPase enzyme, which pumps calcium from the cytoplasm into the SR lumen. × 26,000. Reduced to 70% for publication.

**(B)** Organisation of the junctional SR (JSR) as revealed by freeze-fracture. The junctional SR is continuous with the free SR network; here, two cisternae of junctional SR are illustrated, making intimate contact with a transverse tubule (T). The cisterna to the right of the field has been cross-fractured, while that to the left has been fractured to reveal its membrane *en face*. × 106,000. Reduced to 70% for publication.

**(C)** Thin-section view of junctional SR. The junctional SR cisterna (JSR) contains a calcium-binding protein, calsequestrin, which is seen as conspicuous electron-dense material in the lumen. Release of calcium from this intracellular store stimulates myofibril contraction. Projecting from the junctional SR membrane towards the transverse tubule (T) is a series of electron dense structures, which represent the calcium release channels. × 108,000. Reduced to 70% for publication.

lease channels in the junctional SR facilitates optimal coupling of plasma membrane $Ca^{2+}$ influx to SR $Ca^{2+}$ release into the cytoplasm.

## Cardiomyocyte connections

The membrane machinery we have seen so far allows each myocyte to function as an autonomous contractile unit. To produce a heartbeat, the contractile capabilities of the billions of myocytes that make up the heart have to be mustered in a highly synchronous fashion. This requires both an orderly spread of the wave of electrical activation, and effective transmission of contractile force, from one cell to the next, throughout the heart. To examine the part played by membranes in integrating the activities of individual cells, we now turn our attention to the intercalated disk.

Intercalated disks occur at the blunted ends of each myocyte, joining it to multiple neighbours (Fig. 2A and B). Three types of cell junction—the gap junction, the fascia adherens, and the desmosome—physically connect the disk membranes, acting in concert to integrate cardiac electromechanical function (Fig. 5, central panel). The fascia adherens and desmosome are forms of anchoring junction, responsible respectively for attachment of the myofibrils and the desmin cytoskeleton to sites of cadherin-mediated adhesion between the adjacent plasma membranes. Gap junctions are essentially clusters of channels which span the closely apposed plasma membranes, forming cell-to-cell pathways for rapid conduction of action potentials (our focus here) and direct transmission of chemical signals (of prime importance during development and differentiation.[14-16])

### Gap junctions, connexons, and connexins

With the fundamental dependence of cardiac function on rapid synchronous integration of the activities of individual myocytes very much in mind, Colin Green and I, in the mid-1980s, sought to deepen our understanding of the structural correlates of cardiac gap junction function[17] with new approaches to imaging junctional organisation. A first step was the production of antibodies against the major gap junction protein of the heart, connexin43, first identified by Eric Beyer;[18] another, with the help of Rob Gourdie, was to apply these antibodies effectively for imaging gap-junctional communication pathways by confocal microscopy[19,20] (for reviews see Refs. 19 and 20). Figure 5 uses immunoconfocal imaging, together with thin-section, freeze-fracture and diagrammatic views, to summarise the organisation and structure of the cardiac gap junction, from its distribution in the intercalated disk of a single ventricular myocyte down to the make-up of the individual channels (for review of high resolution structure, see Yeager.[21]) Each cell has multiple disk-clusters of connexin43 gap junctions (Fig. 5A). *En face* images of the disk, made from stacks of serial optical sections in the transverse plane, reveal a ring of large gap junctions at the periphery of the disk encircling numerous smaller junctions[22] (Fig. 5B). The organisation and distribution of the ring-like clusters of gap junctions in the tissue as a whole, together with features of myocyte morphology, result in less resistance to current flow in the longitudinal cell axis than the transverse. One medium-sized "spot" in the *en face* image alone corresponds to an aggregate of many hundreds of channels as seen by freeze-fracture (Fig. 5D). A single channel comprises a pair of coaxially aligned connexons (hemichannels) spanning the narrow extracellular gap (Fig. 5E). Gap-junctional channels are permeable to ions and small molecules up to $\approx$1 kDa in molecular mass, a size that includes second messengers such as inositol triphosphate, cyclic AMP, and $Ca^{2+}$. A single connexon is made from six connexin molecules, the entire channel from twelve. The connexin molecule has four membrane-spanning segments with two extracellular loops, plus a single loop and the amino and carboxyl tails on the cytoplasmic side. The extracellular loops are conserved regions that permit selective docking between connexons. Channel closure may be effected by a change in conformation of the channel protein or, in some instances, by specific domains in the carboxyl tail, which may flip over like a "ball and chain" to block the pore.[23,24] Gating via these mechanisms is regulated by voltage, intracellular pH, calcium concentration, and state of connexin phosphorylation.

Not all connexins are the same; to date, 16 different connexin genes have been identified in mammalian cells[25] (for review see Ref. 25). Most tissues, including those of the heart, express more than one connexin type. As cells stably transfected with cDNAs encoding different connexins show distinct unitary conductance, voltage sensitivity, molecular permeability and ionic selectivity properties, the precise functional properties of gap junctions in vivo would be predicted to depend, at least in part, on the specific connexins from which they are constructed.[26] A key area of interest in my laboratory over the last 10 years has thus been to establish which connexins are expressed where, and how their spatial expression patterns interact, to synchronise proper function in the healthy heart, and with this information, look into the possibility—at first very much a long-shot—that altered gap junction organisation and connexin expression might underlie some of the disturbances of rhythm associated with human heart disease. A prerequisite to tackling these issues was a comprehensive panel of reliable antibody and molecular probes tailored to our needs, a task to which many in the laboratory have contributed, but in which the scientific rigour of Emmanuel Dupont and Steven Coppen has been indispensable.

### Diversity of connexin expression and functional differentiation of cardiomyocytes

Although connexin43 is by far the most abundant connexin in the ventricles and atria of mammalian cardiomyocytes,[27–29] connexin40 and connexin45 are now known also to be locally expressed in specialised zones.[28–30] Apart from specific connexin make-up, variations in size, distribution, and abundance of gap junctions also appear to contribute to the distinctive electrophysiological properties of different myocyte subsets in different regions of the heart.[28,29,31]

The type of myocyte we have focused on so far, the working ventricular cell, is the archetypal cardiomyocyte, responsible for the powerful contractions that constantly pump blood through the vascular system. Their counterparts in the atria, whose action facilitates filling of the ventricles, are modelled on a similar plan, though atrial cells are long and slender, have few or no transverse tubules, and more abundant caveolae, and also, by producing the hormone atrial natriuretic peptide, function as secretory cells.[32] A third somewhat heterogeneous group of myocytes makes up the impulse generation and conduction system—these cells are responsible for generation of the impulse and its precisely timed distribution to the working cells of the chambers at the appropriate point in the cardiac cycle. The cardiac impulse is generated in the sinoatrial (SA) node from where it traverses and activates the atria, before converging on the atrioventricular (AV) node for distribution to the ventricles via a specialised conduction system (His bundle, main bundle branches to each ventricle, and Purkinje fibre network). Myocytes of the impulse generation and conduction system differ morphologically from working myocytes. Those of the nodes are typically small, with a dearth of contractile elements and small, sparse, dispersed gap junctions. These features correlate with poor coupling, which in the sinoatrial node, is linked to the ability to drive the large mass of surrounding atrial tissue while remaining protected from its hyperpolarizing influence, and in the atrioventricular

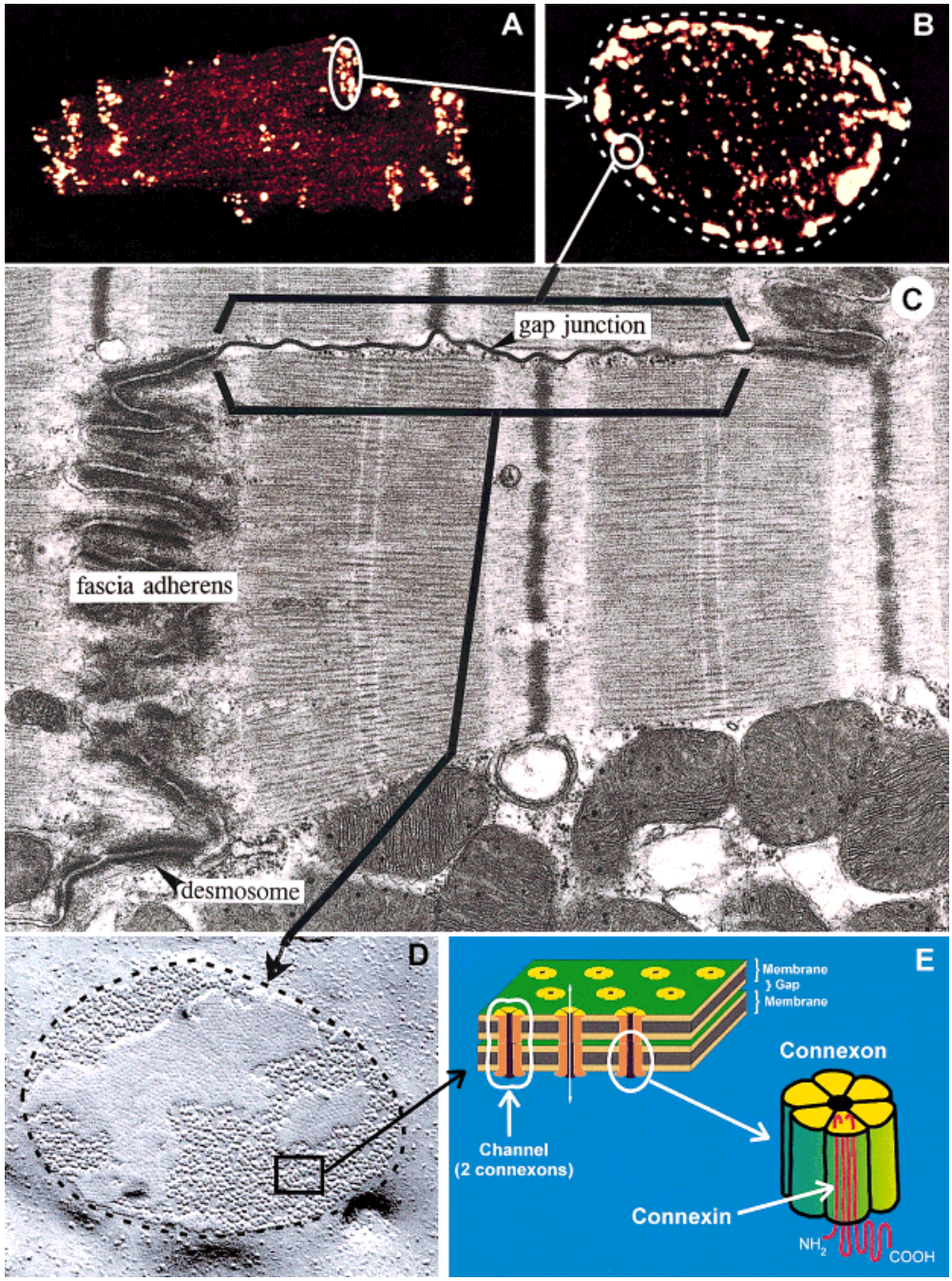


**Figure 5.** The intercalated disk and cardiac gap junction organisation and structure.

**(A)** Clusters of gap junctions at the intercalated disks revealed in a single ventricular cardiac myocyte by immunoconfocal microscopy (connexin43 labelling).

**(B)** One disk-cluster of gap junctions viewed face-on (reconstruction from a stack of serial optical sections). One of these immunolabelled spots corresponds to a single gap junction, as seen by electron microscopy in (C) and (D).

**(C)** Thin-section electron micrograph illustrating the three types of cell junction of the intercalated disk. Gap junctions are recognised where the adjacent plasma membrane profiles run in close contact, separated by a gap of 2 nm. The fascia adherens and the desmosome are characterised by a much wider intermembrane space (≈25 nm) and by prominent electron-dense membrane-associated proteins. The mature intercalated disk appears as a set of irregular steps, with the fasciae adherentes occupying interdigitating transverse regions, and the gap-junctional membrane and most of the desmosomes in the intervening "horizontal" membrane zones, a pattern established during post-natal development.[58,59] × 27,000.

**(D)** Viewing the membrane *en face* by freeze-fracture reveals the gap junction as a cluster of particles (connexons).

**(E)** Each channel consists of two connexons, and each connexon of six connexins. Different types of connexin are denoted using a suffix indicating the molecular mass. The principal amino acid sequence differences between connexins occur in the carboxyl tail, a region involved in regulation of channel properties. Compatibility between connexons composed of different connexin types is determined by the sequence of the second extracellular loop, as well as by specific intracellular domains.

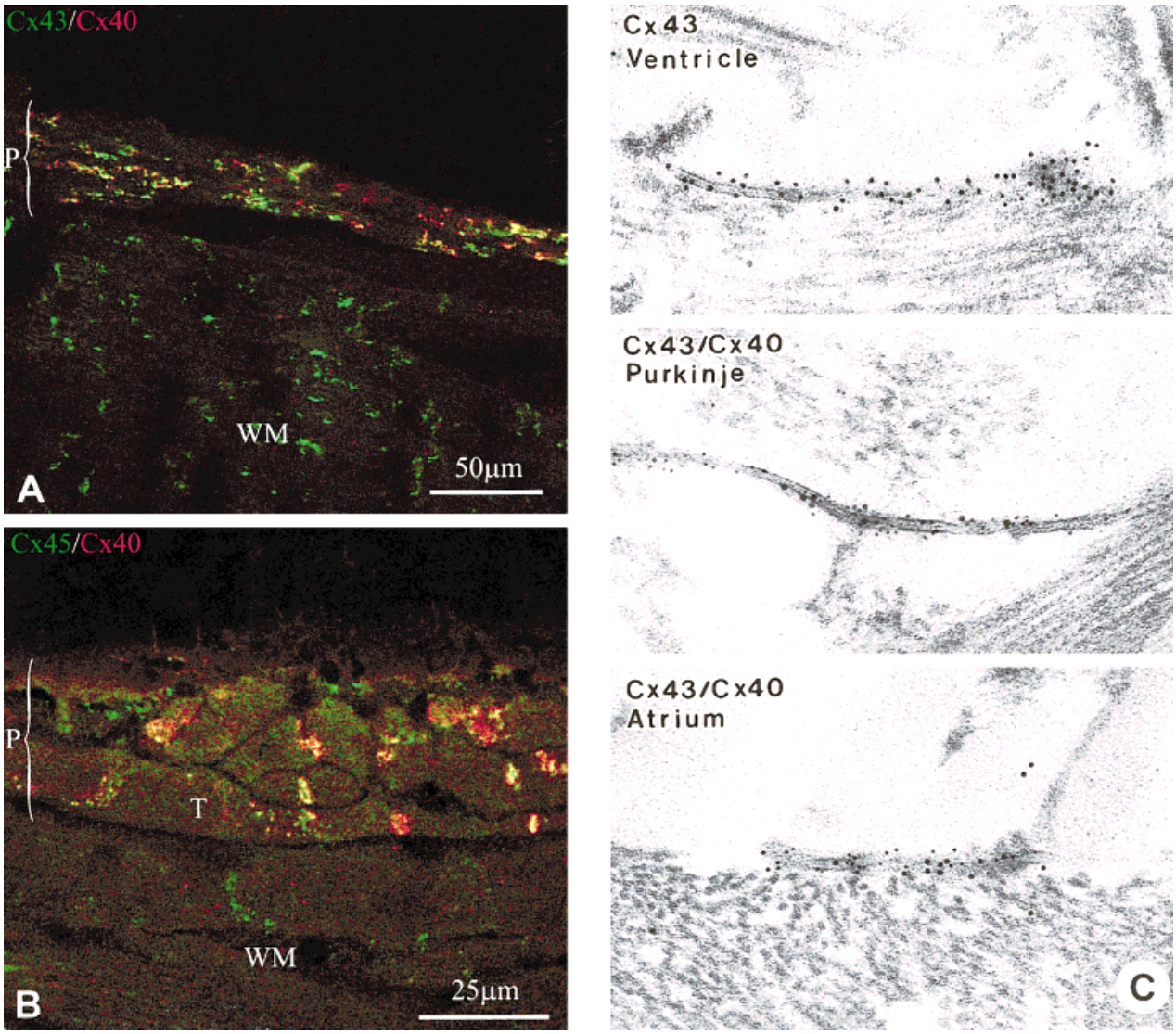


**Figure 6.** Spatial distribution of connexins 43, 40, and 45.

**(A & B)** Immunoconfocal microscopy of mouse Purkinje fibre. (A) The Purkinje fibre (P) shows prominent immunolabelling for connexin40 (red) and connexin43 (green), the yellow fluorescence indicating sites of colocalization of the two connexins. The working myocardium (WM) expresses connexin43, but no detectable connexin40. (B) connexin45 is expressed with connexin40 in the Purkinje fibre (P), but is undetectable or barely detectable in working myocardium (WM). T indicates transitional cell which connects Purkinje cells to working myocytes. (Micrographs by Steven Coppen).

**(C)** Multiple immunogold labelling for electron microscopy, using two distinct sizes of gold marker to discriminate connexin43 and connexin40, demonstrates that when two connexins are co-expressed, they are frequently present as mixtures within individual gap junctions. Gap junctions between working ventricular myocytes (rat) show intense immunogold label for connexin43, but not connexin40; gap junctions between Purkinje cells (rat) and right atrial muscle cells (human) show positive labelling for both connexin43 (small gold markers) and connexin40 (larger gold). (Micrographs by Stephen Rothery). × 91,000.

node, to a slowing of conduction which ensures sequential contraction of atria and ventricles.

The ability of the Purkinje fibre system to distribute the impulse rapidly throughout the working ventricular myocardium correlates with large, abundant gap junctions and with high levels of connexin40,[33] a connexin that gives high conductance channels[34] (Fig. 6). Working ventricular myocytes characteristically lack connexin40, though this connexin is

present in the atrial myocytes of most species[35] (Fig. 6). Connexin45, a connexin that forms low conductance channels,[36] is present only in very small quantities; this connexin is typically undetectable or barely detectable in working ventricular myocytes, though slightly higher levels are present in the atrium.[30,35] In the rodent ventricle, connexin45 is predominantly expressed in the conduction system where it co-localizes with connexin40 (Fig. 6). These two connexins are the main constituents of the very small gap junctions both of the atrioventricular and sino-atrial node. In the rat conduction system, the zone of connexin40/connexin45 co-expression forms a subcompartment enveloped by a zone in which only connexin45 is found.[37] The presence of connexin45 continuously through the ventricular conduction system explains how impulse conduction through this system is maintained (albeit with conduction abnormalities) in the connexin40 knockout mouse.[37–39] In the SA node of the rabbit, the connexin43 negative node is clearly delineated from the surrounding atrial myocardium except for a restricted zone of connexin45/connexin43 co-expression at the nodal/crista terminalis border—a candidate pathway for directed exit of the impulse from the node into the atrial tissue.[40]

These examples illustrate how spatial expression of connexins of different intercellular coupling properties and compatibilities may permit selective communication between functionally distinct tissue compartments. Not all connexin combinations are compatible (i.e., capable of forming functional channels); a connexin40 connexon, for example, cannot dock with a connexin43 connexon, whereas a connexin45 connexon can dock with either.[26] The presence of connexin45 in transitional zones between the impulse generation/conduction system and working myocardium is thus of interest because of the potential ability of this connexin to link otherwise incompatible connexin43 and connexin40 expressing zones. In cells expressing more than one connexin type, however, a multiplicity of different arrangements involving heterotypic channels (those comprising a connexon made from one connexin type connected to a connexon made from a different connexin type), homotypic channels (in which a single connexin type is present), or heteromeric channels (in which the connexon itself contains a mixture of connexins) is possible, the functional correlates of which are yet to be unravelled. Interestingly, some heterotypic combinations of connexon (including those involving connexin43 and connexin45) show asymmetric voltage dependence, a property associated with rectifying channels[26], though whether such one-directional channels play a role in current spread in vivo in the heart is not yet known.

### Gap junctions, heart disease, and arrhythmia

As we have seen, gap junctions mediate the orderly cell-to-cell transmission of the action potentials that govern regular synchronous contraction in the healthy heart. Derangements of gap junctions, in addition to altered membrane excitability, could thus in principle contribute to the dangerous disturbances of heart rhythm (arrhythmias) found in heart disease.[41] Most ventricular arrhythmias in human heart disease are due to reentrant electrical circuits (where the impulse describes a self-perpetuating "circus" course). Macro-reentry circuits can arise from a "freak" gap junction-coupled strand of tissue between the atrium and ventricle that bypasses the atrioventricular node, a condition termed Wolff-Parkinson White syndrome.[42] The micro-reentry arrhythmias common in patients with hypertrophic and ischaemic heart disease (the common form of heart disease caused by coronary artery blockage) are precipitated by abnormally slow conduction, heterogeneous wavefront propagation, and localized uni-directional block, due to reduced gap-junctional coupling, reduced membrane excitability and/or altered tissue architecture.[43,44] Two forms of gap junction abnormality we have identified in human heart disease potentially contribute to such pro-arrhythmic conditions—localized disordering of gap junction distribution at the border zone of infarcts and down-regulation of connexin43[41,45] (for reviews see Refs. 41 and 45).

Where non-fatal myocardial infarction (death and scarring of a portion of heart tissue) occurs in ischaemic heart disease, loss of the normal ordered distribution of connexin43 gap junctions is conspicuous in the myocardial zone bordering infarct scar tissue.[46] Gap junctions in these zones are scattered extensively over the lateral borders of the cells, while those at more distant sites remain in clearly ordered intercalated disk arrays. Abnormal gap junction distributions of this type are not solely related to late stages in myocardial degeneration or remodelling associated with fibrosis, but are detectable within a few days after myocardial infarction in the dog.[47] By using high resolution electrode arrays to map reentrant circuits in the epicardial border zone overlying 4-day old infarcts in this model, and then mapping gap junction distribution in precisely the same zones by immunoconfocal microscopy, Nick Peters elegantly demonstrated that regions of full thickness gap junction disarray correspond spatially to the common central pathway of figure-of-eight re-entrant circuits.[47] We have also identified abnormal patterns of gap junction distribution in other human cardiac abnormalities associated with an increased arrhythmic tendency, notably hypertrophic cardiomyopathy.[48]

In addition to disrupted patterns of gap junction organisation in the immediate vicinity of the infarct, quantitative immunoconfocal microscopy reveals a generalised decrease in immunolabelled connexin43 gap junction content per myocyte throughout the left ventricular myocardium of patients with ischaemic heart disease.[49] Decreased levels of connexin43 transcripts and protein are correspondingly

found by northern and western blotting.[50] That reduced levels of connexin43 are sufficient to cause slowed ventricular conduction has been reported in mice heterozygous for a null mutation in the connexin43 gene.[51] In human ischaemic heart disease, reduced levels of immunodetectable connexin43 are found both in regions of the ventricle subject to reversible (exercise-induced) ischaemia[49] and in "hibernating" regions.[52] "Hibernation" defines a state of impaired contractile function in which the myocytes remain viable, with the potential for recovery after coronary by-pass surgery. The reduction in immunolabelled gap junctions is greater in hibernating myocardium than in reversibly ischaemic myocardium, with preferential loss of the large gap junctions at the disk periphery. Prognosis in medically treated patients with ischaemic heart disease and impaired ventricular function is poorer when there is evidence of hibernation in addition to reversible ischaemia, and the majority of these cardiac deaths are sudden, again reinforcing a link between reduced connexin43 levels and arrhythmia.

The concept that altered connexin43 expression contributes to arrhythmia in human heart disease raises the issue of the gap junction as a potential therapeutic target. Before the feasibility of such a speculative prospect can be realistically assessed, we need to know more—a great deal more. One priority is comprehensive information on the functional properties of the different patterns of multiple connexin expression found in the healthy heart; another is to determine whether expression of connexins other than connexin43 is altered in disease. On a parallel front, emerging data on vascular cell connexins[53–57] highlights the potential importance of gap-junctional communication in genesis of the primary vascular lesion of coronary heart disease.

## Concluding comment

Our understanding of how the cardiac muscle cell works owes much to the integration of morphological findings with those from physiology and cell/molecular biology. As highlighted here, results from modern cellular imaging techniques have been pivotal to the ideas that spatially-defined patterns of expression of different connexins underlie the precisely orchestrated patterns of current flow governing the normal heart rhythm, and that one cause of arrhythmia in heart disease lies in altered gap junction organisation and connexin expression. These examples remind us that, in an era where approaches other than the structural are in the ascendant, there remains a need for sophisticated techniques for localization of gene products and high resolution cellular imaging as part of a multidisciplinary approach to understanding cardiac function in health and disease.

## Acknowledgments

I thank the British Heart Foundation and the Wellcome Trust for support, and all those who have contributed to the work discussed, in particular Colin Green, Rob Gourdie, Stephen Rothery, Nick Peters, Emmanuel Dupont, Steven Coppen, Hung-I Yeh, Raffi Kaprielian, Yu-Shien Ko, Shirley Stevenson, Yoshiko Takagishi, David Gathercole, Elizabeth Harfst, Jonathan Smith, and Jim Blackburn.

## Note added in proof

In contrast to the page by Guerrero et al.[51] cited in the discussion above, a recent study on the heterozygous ($Cx43^{+/-}$) mouse reports no alteration in ventricular conduction velocities (or ECG parameters) compared with the wordtype mouse (Morley, G.E. et al. J Cardiovasc Electrophysiol 1999;10:1361–1375).

## References

1. Severs NJ, Shotton DM. Rapid freezing, freeze fracture, and deep etching. New York: Wiley Liss; 1995. p 1–372.
2. Weissmann G, Claiborne R. Cell Membranes. Biochemistry, cell biology and pathology. New York: HP Publishing Company. 1975; p 1–383.
3. Hayat MA. Colloidal gold: principles, methods and applications. Volumes 1-3. New York: Academic Press; 1991.
4. Echlin P. Low-temperature microscopy and analysis. New York: Plenum Pub. Corp.; 1992.
5. Severs NJ. Freeze-fracture cytochemistry: an explanatory survey of methods. In: Severs NJ, Shotton DM, editors. Rapid freezing, freeze fracture, and deep etching. New York: Wiley-Liss Inc.; 1995. p 173–208.
6. Fujimoto K. SDS-digested freeze-fracture replica labeling electron microscopy to study the two-dimensional distribution of integral membrane proteins and phospholipids in biomembrane: practical procedure, interpretation and application. Histochem Cell Biol 1997;107:87–96.
7. Sheppard CJR, Shotton DM. Confocal laser scanning microscopy. Royal Microscopical Society Microscopy Handbook No.38. Oxford: BIOS Scientific Publishers; 1997. p 1–106.
8. Stevenson S, Rothery S, Cullen MJ, Severs NJ. Dystrophin is not a specific component of the cardiac costamere. Circ Res 1997;80:269–280.
9. Stevenson S, Rothery S, Cullen MJ, Severs NJ. Spatial relationship of C-terminal domains of dystrophin and Beta-dystroglycan in cardiac muscle support a direct molecular interaction at the plasma membrane interface. Circ Res 1998;82:82–93.
10. Severs NJ. Cholesterol cytochemistry in cell biology and disease. In: Bittman R, editor. Subcellular biochemistry. Volume 28. Cholesterol: its functions and metabolism in biology and medicine. London: Plenum Press; 1997. p 477–505.
11. Page E, Winterfield J, Goings G, Bastawrous A, Upshaw-Earley J, Doyle D. Water channel proteins in rat cardiac myocyte caveolae: osmolarity-dependent reversible internalization. Am J Physiol (Heart Circ Physiol) 1998;274: H1988–H2000.
12. Takagishi Y, Rothery S, Issberner J, Levi AJ, Severs NJ. Spatial distribution of dihydropyridine receptors in the plasma membrane of guinea pig cardiac myocytes investigated by correlative confocal microscopy and label-fracture electron microscopy. J Electron Microsc 1997;46:165–170.
13. Gathercole DV, Colling DJ, Takagishi Y, Skepper JN, Levi AJ, Severs NJ. L-type $Ca^{2+}$ calcium channel clusters over junctional sarcoplasmic reticulum in guinea pig cardiac myocyte. J Mol Cell Cardiol 1999;31:pA106:(Abstract).
14. Britz-Cunningham SH, Shah MM, Zuppan CW, Fletcher WH. Mutations of the *connexin43* gap-junction gene in patients with heart malformations and defects of laterality. N Engl J Med 1995;332:1323–1329.
15. Gourdie RG, Litchenberg WH, Eisenberg LM. Gap junctions and heart development. In: De Mello WC, editor. Heart cell communication in health and disease. Kluwer; 1998. p 19–44.
16. Sullivan R, Huang GY, Meyer RA, Wessels A, Linask KK, Lo CW. Heart malformations in transgenic mice exhibiting dominant negative inhibition of gap junctional communication in neural crest cells. Dev Biol 1998;204:224–234.

17. Green CR, Severs NJ. Gap junction connexon configuration in rapidly frozen myocardium and isolated intercalated disks. J Cell Biol 1984;99:453–463.
18. Beyer EC, Paul DL, Goodenough DA. Connexin43: a protein from rat heart homologous to a gap junction protein from liver. J Cell Biol 1987;105:2621–2629.
19. Green CR, Severs NJ. Distribution and role of gap junctions in normal myocardium and human ischaemic heart disease. Histochemistry 1993;99:105–120.
20. Severs NJ, Gourdie RG, Harfst E, Peters NS, Green CR. Review. Intercellular junctions and the application of microscopical techniques: the cardiac gap junction as a case model. J Microsc 1993;169:299–328.
21. Yeager M. Structure of cardiac gap junction intercellular channels. J Struct Biol 1998;121:231–245.
22. Gourdie RG, Green CR, Severs NJ. Gap junction distribution in adult mammalian myocardium revealed by an antipeptide antibody and laser scanning confocal microscopy. J Cell Sci 1991;99:41–55.
23. Unwin PNT, Ennis PD. Two configurations of a channel-forming membrane protein. Nature 1984;307:609–613.
24. Morley GE, Ek-Vitorin JF, Taffet SM, Delmar M. Structure of connexin43 and its regulation by pHi. J Cardiovasc Electrophysiol 1997;8:939–951.
25. Cardew G. Gap junction-mediated intercellular signalling in health and disease. New York: John Wiley & Son; 1999. p 1–285.
26. Bruzzone R, White TW, Goodenough DA. The cellular internet: on-line with connexins. BioEssays 1996;18:709–718.
27. Beyer EC, Kistler J, Paul DL, Goodenough DA. Antisera directed against connexin43 peptides react with a 43-kd protein localized to gap junctions in myocardium and other tissues. J Cell Biol 1989;108:595–605.
28. Gros DB, Jongsma HJ. Connexins in mammalian heart function. BioEssays 1996;18:719–730.
29. Severs NJ, Dupont E, Kaprielian RR, Yeh H-I, Rothery S. Gap junctions and connexins in the cardiovascular system. In: Yacoub MH, Carpentier A, Pepper J, Fabiani J-N editors. Annual of cardiac surgery 1996: 9th edition. London: Current Science; 1996. p 31–44.
30. Coppen SR, Dupont E, Rothery S, Severs NJ. Connexin45 expression is preferentially associated with the ventricular conduction system in mouse and rat heart. Circ Res 1998;82:232–243.
31. Saffitz JE, Beyer EC, Darrow BJ, Guerrero PA, Beardslee MA, Dodge SM. Gap junction structure, conduction, and arrhythmogenesis: direction for future research. In: Spooner PM, Joyner RW, Jalife J, editors. Discontinuous conduction in the heart. New York: Futura Publishing Company; 1997. p 89–105.
32. Newman TM, Severs NJ. Effect of neuromimetics upon the release of atrial natriuretic peptide granules: are multiple pathways involved in secretion. J Cell Physiol 1996;168:134–140.
33. Gourdie RG, Severs NJ, Green CR, Rothery S, Germroth P, Thompson RP. The spatial distribution and relative abundance of gap-junctional connexin40 and connexin43 correlate to functional properties of the cardiac atrioventricular conduction system. J Cell Sci 1993;105:985–991.
34. Elfgang C, Eckert R, Lichtenberg-Fraté H, Butterweck A, Traub O, Klein RA, Hülser DF, Willecke K. Specific permeability and selective formation of gap junction channels in connexin-transfected HeLa cells. J Cell Biol 1995;129:805–817.
35. Vozzi C, Dupont E, Coppen SR, Yeh H-I, Severs NJ. Chamber-related differences in connexin expression in the human heart. J Mol Cell Cardiol 1999;31:991–1003.
36. Moreno AL, Laing JG, Beyer EC, Spray DC. Properties of gap junction channels formed of connexin 45 endogenously expressed in human hepatoma (SKHep1) cells. Am J Physiol (Cell Physiol) 1995;268:C356–C365.
37. Coppen SR, Severs NJ, Gourdie RG. Connexin45 ($\alpha$6) expression delineates an extended conduction system in the embryonic and mature rodent heart. Dev Genet 1999;24:82–90.
38. Kirchhoff S, Nelles E, Hagendorff A, Kruger O, Traub O, Willecke K. Reduced cardiac conduction velocity and predisposition to arrhythmias in connexi40-deficient mice. Curr Biol 1998;8:299–302.
39. Simon AM, Goodenough DA, Paul DL. Mice lacking connexin40 have cardiac conduction abnormalities characteristic of atrioventricular block and bundle branch block. Curr Biol 1998;8:295–298.
40. Coppen SR, Kodama I, Boyett MR, Dobrzynski H, Takagishi Y, Honjo H, Yeh H-I, Severs NJ. Connexin45, a major connexin of the rabbit sinoatrial node, is co-expressed with connexin43 in a restricted zone at the nodal-crista terminalis border. J Histochem Cytochem 1999;47:907–918.
41. Severs NJ. Cardiovascular disease. In: Cardew G, editor. Gap junction-mediated intercellular signalling in health and disease. New York: John Wiley & Sons; 1999. p 188–206.
42. Peters NS, Rowland E, Bennett JG, Green CR, Anderson RH, Severs NJ. The Wolff-Parkinson-White syndrome: the cellular substrate for conduction in the accessory atrioventricular pathway. Eur Heart J 1994;15:981–987.
43. Shaw RM, Rudy Y. Ionic mechanisms of propagation in cardiac tissue—roles of the sodium and L-type calcium currents during reduced excitability and decreased gap junction coupling. Circ Res 1997;81:727–741.
44. Rohr S, Kucera JP, Kleber AG. Slow conduction in cardiac tissue, I: effects of a reduction of excitability versus a reduction of electrical coupling on microconduction. Circ Res 1998;83:781–794.
45. Severs NJ. Gap junctions and coronary heart disease. In: De Mello WC, Janse MJ, editor. Heart cell communication in health and disease. Boston: Kluwer; 1998. p 175–194.
46. Smith JH, Green CR, Peters NS, Rothery S, Severs NJ. Altered patterns of gap junction distribution in ischemic heart disease. An immunohistochemical study of human myocardium using laser scanning confocal microscopy. Am J Pathol 1991;139:801–821.
47. Peters NS, Severs NJ, Coromilas J, Wit AL. Disturbed connexin43 gap junction distribution correlates with the location of reentrant circuits in the epicardial border zone of healing canine infarcts that cause ventricular tachycardia. Circulation 1997;95:988–996.
48. Sepp R, Severs NJ, Gourdie RG. Altered patterns of cardiac intercellular junction distribution in hypertrophic cardiomyopathy. Heart 1996;76:412–417.
49. Peters NS, Green CR, Poole-Wilson PA, Severs NJ. Reduced content of connexin43 gap junctions in ventricular myocardium from hypertrophied and ischaemic human hearts. Circulation 1993;88:864–875.
50. Dupont E, Vozzi C, Coppen SR, Kaprielian RR, Severs NJ. Connexin mRNA and protein expression is altered in human heart disease. J Mol Cell Cardiol 1997;29:A108. (Abstract)
51. Guerrero PA, Schuessler RB, Davis LM, Beyer EC, Johnson CM, Yamada KA, Saffitz JE. Slow ventricular conduction in mice heterozygous for connexin43 null mutation. J Clin Invest 1997;99:1991–1998.
52. Kaprielian RR, Gunning M, Dupont E, Sheppard MN, Rothery SM, Underwood R, Pennell DJ, Fox K, Pepper J, Poole-Wilson PA, Severs NJ. Downregulation of immunodetectable connexin43 and decreased gap junction size in the pathogenesis of chronic hibernation in the human left ventricle. Circulation 1998;97:651–660.
53. Blackburn JP, Peters NS, Yeh H-I, Rothery S, Green CR, Severs NJ. Upregulation of connexin43 gap junctions during early stages of human coronary atherosclerosis. Arterioscler Thromb Vasc Biol 1995;15:1219–1228.
54. Yeh H-I, Lupu F, Dupont E, Severs NJ. Upregulation of connexin43 gap junctions between smooth muscle cells after balloon catheter injury in the rat carotid artery. Arterioscler Thromb Vasc Biol 1997;17:3174–3184.
55. Yeh H-I, Dupont E, Rothery S, Coppen SR, Severs NJ. Individual gap junction plaques contain multiple connexins in arterial endothelium. Circ Res 1998;83:1248–1263.
56. Ko Y-S, Yeh H-I, Haw M, Dupont E, Kaba R, Plenz G, Robenek H, Severs NJ. Differential expression of connexin43 and desmin defines two subpopulations of medial smooth muscle cells in the human internal mammary artery. Arterioscler Thromb Vasc Biol 1999;19:1669–1680.
57. Ko Y-S, Yeh H-I, Rothery S, Dupont E, Coppen SR, Severs NJ. Connexin make-up of endothelial gap junctions in the rat pulmonary artery as revealed by immunoconfocal microscopy and triple-label immunogold electron microscopy. J Histochem Cytochem 1999;47:683–692.
58. Angst BD, Khan LUR, Severs NJ, Whitely K, Rothery S, Thompson RP, Magee AI, Gourdie RG. Dissociated spatial patterning of gap junctions and cell adhesion junctions during postnatal differentiation of ventricular myocardium. Circ Res 1997;80:88–94.
59. Peters NS, Severs NJ, Rothery SM, Lincoln C, Yacoub MH, Green CR. Spatiotemporal relation between gap junctions and fascia adherens junctions during postnatal development of human ventricular myocardium. Circulation 1994;90:713–725.